

Influence of heat treatment on the micro/nano-tribological properties of ultra-thin ionic liquid films on silicon

Wenjie Zhao^{a,b}, Ying Wang^{a,b}, Liping Wang^{a,*}, Mingwu Bai^c, Qunji Xue^a

^a State Key Laboratory of Solid Lubrication, Lanzhou Institute of Chemical Physics, Chinese Academy of Sciences, Lanzhou 730000, China

^b Graduate School of Chinese Academy of Sciences, Beijing 100039, China

^c Department of Mechanical & Aerospace Engineering, George Washington University, Ashburn, VA20147, USA

ARTICLE INFO

Article history:

Received 16 December 2009

Received in revised form 12 February 2010

Accepted 14 March 2010

Available online 20 March 2010

Keywords:

Micro/nano-friction

Adhesion

RTIL

Heat treatment

AFM

ABSTRACT

The performance of micro- and nano-electromechanical systems (M/NEMS) depends on the surface and interface properties of the substrate, such as chemical composition, roughness, friction, adhesion, and wear. In order to solve these problems and improve the performance of M/NEMS, molecularly thin films of room temperature ionic liquid (RTIL)-1,3-di(2-hydroxyethyl)imidazolium hexafluorophosphate which has two terminal hydroxyl groups were prepared on silicon substrate. Thermal stability of the RTIL was evaluated using thermogravimetric analysis in a nitrogen atmosphere. A multi-functional X-ray photoelectron spectrometer was used to investigate the chemical compositions of the films. The morphology, nano-friction and nano-adhesion properties of RTIL films with different heat treatment were experimentally investigated at nanoscale using atomic force microscopy/friction force microscopy. The wear-resistant property was tested on a ball-on-plate microtribometer. The results revealed that the micro/nano-friction and adhesion properties of RTIL films were significantly improved with appropriate heat treatment. The corresponding friction reduction and anti-adhesion mechanisms of the tested ultra-thin RTIL films under tested condition were proposed based on the experimental observations. For the micro/nano-friction, bonding ratio of the lubricant film had great effect on the RTIL's performance.

© 2010 Elsevier B.V. All rights reserved.

1. Introduction

With the appearance of micro/nanostructures and increasing demand for miniaturization of moving components in nano-technological devices, such as magnetic storage devices and micro/nano-electromechanical systems (M/NEMS), tribological properties at nanoscale between two sliding surfaces have attracted much attention as they significantly affect the performance and reliability of microdevices [1,2]. The surfaces between M/NEMS are generally separated by a few nanometers [3,4], accordingly, adhesion, friction and stiction at nanoscale become critical and can be detrimental to the efficiency, power output and reliability of M/NEMS devices [5,6].

An ultra-thin organic film as a boundary lubricant is very important to many modern technologies including magnetic storage devices and M/NEMS [2,7]. Perfluoropolyethers (PFPEs) have been commonly used as lubricating films in M/NEMS and magnetic disk drive industry to reduce the friction and wear of the interface [8–10] because they have many unique properties

such as very low vapor pressure, good chemical and thermal stability, low surface tension and high contact angle. However, PFPEs are catalytically degraded by strong nucleophilic agents and strong electropositive metals, which together with the high cost of PFPEs, limit their application in some fields [11–13]. Therefore, the development of new alternatives to PFPEs is essential.

Room temperature ionic liquids (RTILs) have awakened big interest due to their unique chemical and physical properties, such as negligible vapor pressures, non-flammability, high thermal stability, low melting point, broad liquid range, and a highly solvating capacity for both polar and nonpolar compounds. Their strong electrostatic bonding compared to covalently bonded fluids leads to very desirable lubrication properties [6]. Thus they are considered as lubricants for M/NEMS. So far, only macroscale friction and wear tests have been conducted on these materials. Ye et al. investigated the tribological behaviors of two kinds of alkylimidazolium RTILs, and found them promising versatile lubricants for many frictional pairs such as steel/steel, steel/aluminum, steel/copper, steel/silicon, steel/sialon ceramics in the macroscale [14]. Liu and co-workers have performed laboratory tribological tests on other alkylimidazolium base RTILs and proved them superior to traditional lubricants – such as X-1P, PFPE, and ZDDP

* Corresponding author. Tel.: +86 931 4968080; fax: +86 931 4968163.
E-mail address: lpwang@licp.cas.cn (L. Wang).

– in terms of friction reduction, anti-wear performance and load-carrying capacity [15–19].

Adhesion and friction properties at the micro/nanoscale are different from the macroscale [20]. Recently, extensive laboratory studies have been conducted to examine the nano-tribological properties of RTILs applied as ultra-thin film (about 2 nm) on a polished silicon or DLC surface, which is considered to be crucial to understand how these novel films can efficiently lubricate M/NEMS devices [21–24]. Our group carried out earlier research on micro/nano-tribological properties of ultra-thin RTILs films and have investigated effect of the anion and cation on the nano-tribological properties of several kinds of RTILs nano-films [22,25–29]. However, the influence of heat treatment on micro/nano-tribological behavior of RTIL films directly deposited on silicon surface has not been examined yet. This work presents a systematic study of the micro/nano-tribological behaviors of RTIL focused on heat treatment effects. It is aimed to acquire insights into their potential in resolving the tribological problems of M/NEMS. 1,3-di(2-hydroxyethyl)imidazolium hexafluorophosphate was carefully chosen due to two beneficial effects of the unique properties of both cation and anion. Firstly, the RTIL-cation possesses two OH-groups. Therefore, RTIL binds to the hydroxylated silicon surface via the condensation reaction of the functional OH-groups of the RTIL-cation with hydroxylated silicon surface. Secondly, the RTIL anion hexafluorophosphate (PF₆⁻) has showed better micro/nano-tribological performance than other anions [22,25–27]. In this work, the lubricant adsorbed onto silicon after the solvent rinsing process, which is termed as bonding lubricant.

2. Experimental details

2.1. Materials

P-doped single side polished single-crystal silicon (100) wafers (obtained from GRINM Semiconductor Materials Co. Ltd., Beijing) with a surface roughness of about 0.2 nm and a thickness of 0.5 mm were used as the substrate. Functionalized RTIL: 1,3-di(2-hydroxyethyl)imidazolium hexafluorophosphate, marked as IL-OH, was synthesized using the similar procedures as described in Refs. [30,31]. All other reagents were of analytical grade and used as received without any further purification. The chemical structure of the RTIL used in this study is given in Fig. 1.

2.2. Preparation of RTIL films

All glass vials used in this experiment were cleaned by thoroughly rinsing with deionized (DI) water and acetone and then dried at 100 °C in an oven. Cleaned silicon wafers were immersed in a freshly prepared Piranha solution (volume ratio of 7:3 mixture of 98% H₂SO₄ and 30% H₂O₂) at 90 °C for 40 min to produce hydroxyl groups on the surfaces, and this kind of silicon was abbreviated as Si-OH. Then the substrates were rinsed with DI water and blown dry with nitrogen flow. Solutions of IL-OH were prepared in acetone at different concentrations ranges from 0.2 to 1.0 mg/mL. The silicon wafer was slowly dipped into a tank containing the solu-

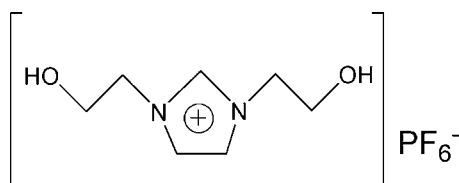


Fig. 1. Chemical structure of the IL-OH molecule.

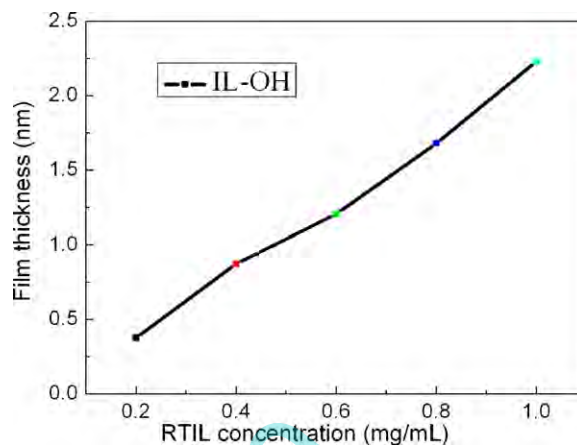


Fig. 2. Plots of film thickness as function of IL-OH solution concentration at a pull-off velocity of 60 μm/s.

tion and then withdrawn from it with a velocity of 60 μm/s after being immersed in the solution for 2 min. Si wafer was allowed to dry in air in a clean room prior to the following measurements. As shown in Fig. 2, the thickness of the films is in proportion to the concentration of the solution. According to this relationship, it is easy to prepare RTIL films with a certain thickness. In order to compare the nano-tribological properties of RTIL with different heat treatment, the thickness of all the films we made in this article is about 2 nm. Consequently, the final RTIL concentration used for the required film thickness of 2 nm is 0.9 mg/mL. Then the RTIL films were heated at 60 and 120 °C for 1 h, respectively, which were designated as IL-OH-60 and IL-OH-120. At last, some of IL-OH-120 films were rinsed and washed ultrasonically with excess acetone (twice) to remove excess and physisorbed IL-OH molecules. This kind of film was designated as IL-OH-120-clean.

2.3. Characterization of films

An L116-E ellipsometer (Gaertner, USA) equipped with a He-Ne laser ($\lambda = 632.8$ nm) at a fixed incidence angle of 50° was used to measure the film thickness. The thickness was recorded at an accuracy of ± 0.3 nm from 10 locations on each sample.

A PHI-5702 multi-functional X-ray photoelectron spectrometer (XPS), was applied for the determination of the chemical compositions and structures of the surfaces coated with RTIL. As parameters, a pass energy of 29.35 eV, Mg-K α ($h = 1253.6$ eV) radiation for excitation and a take off angle of 36° were used. Chamber pressure was about 3×10^{-8} Torr. The binding energy of contaminating carbon of C1s at 284.8 eV was used as the reference.

2.4. Measurement of nano-friction and nano-adhesion characteristics

AFM/FFM is widely used in nanotribology and nanomechanics studies. In this study, surface morphologies and nano-tribological behaviors of RTIL films were characterized with an AFM/FFM controlled by CSPM4000 electronics made by Benyuan, China, using the contact mode. Commercially available triangular Si₃N₄ cantilever (CSC21/Si₃N₄/Al BS, overall Si₃N₄ coating, backside Al-coated) with a nominal spring constant of 2 N/m and a Si₃N₄ tip with a radius of curvature about 10 nm was employed.

To study frictional properties of the surfaces, a variation of torsion deflections (a friction loop) were detected according to the well established protocol [32,33]. The tip was scanned back and forth in the x direction in contact with sample at a constant load while the lateral deflection of the lever was measured. The differ-

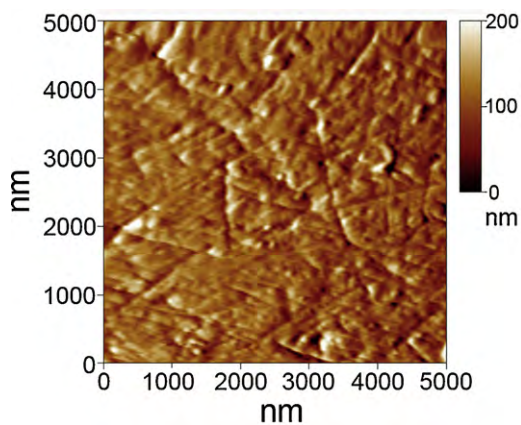


Fig. 3. AFM topography of the Si_3N_4 ball surface.

ence in the lateral deflection or friction signal between back and forth motions is proportional to the friction force. Friction forces were continuously measured with various external loads. The load was increased linearly in each successive scan line ranging from 12 to 180 nN automatically controlled by computer software. Scanning for the friction force measurement was performed at rate of 1 Hz along the scan axis and a scan size of $1\ \mu\text{m} \times 1\ \mu\text{m}$. The scan axis was perpendicular to the longitudinal direction of the cantilever. The sets of data were displayed graphically in a friction image.

For the comparison to be valid, the same cantilever/tip was used during the experiment unless specified otherwise. Furthermore, to avoid the influence of molecules which may transfer to the tip during the AFM/FFM experiment, the tip was scanned on a cleaved mica surface to remove these physically adsorbed molecules. Each presented curve represents an average over at least 10 different measurements. All the experiments were performed at a relative humidity level of 30–40% at room temperature.

AFM has been also used extensively to measure adhesive forces between surfaces at the nanoscale. The adhesive force (F) which is also called pull-off force was calculated by $F = K_c Z_p$ [9,34], where K_c is the force constant of cantilever and Z_p is the maximum vertical displacement of the piezotube.

2.5. Micro-friction and wear study

The microtribology and anti-wear properties of all these RTIL films were evaluated using a UMT-2MT microtribometer operating in the reciprocating mode. A Si_3N_4 ball of 3.18 mm in diameter was selected as the counterpart. Fig. 3 shows the surface morphology of the Si_3N_4 ball used in this study. The root-mean-square (RMS) roughness of the ball was estimated to be about 28.6 nm. The Si_3N_4 ball was fixed in a stationary holder sustained by a beam and the samples were then mounted on a reciprocating table. The ball moved horizontally with respect to the sample surface with a sliding frequency of 1 Hz and a stroke of 5 mm. Applied normal loads used were between 60 and 200 mN and the change in the friction coefficient was monitored versus sliding time or cycles. The initiation of wear on the sample surface leads to an increase in the friction coefficient, and a sharp increase was interpreted to indicate film failure. The friction coefficient and sliding times were recorded automatically by a computer, and at least three repeated measurements were performed. A schematic illustration of the microtribometer is shown in Fig. 4. All the tests were conducted at room temperature and at a relative humidity of 30–40%.

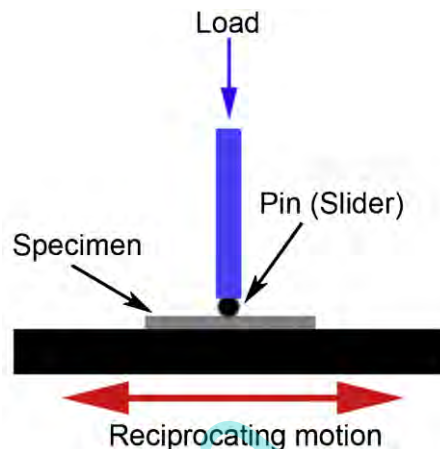


Fig. 4. Schematic illustration of pin-on-plate microtribometer.

3. Results and discussion

3.1. Thermal behavior IL-OH

Thermal stability of IL-OH was examined by thermogravimetric analysis (TGA) between 20 and 800 °C, a constant heating rate of 10°/min and high-purity nitrogen purge was used for all the measurements. As shown in Fig. 5, IL-OH showed little weight loss below 200 °C, which corresponds to the extremely low vapor pressures of RTIL and hence meets the demand of high performance lubricant. Further, it is observed that thermal degradation of IL-OH starts at 200 °C and is completed at 400 °C. IL-OH showed good performance in terms of thermal stability which was nearly comparable to Zdol.

3.2. Composition and morphology

The X-ray photoelectron spectroscopy data of surfaces were used to characterize the chemical states of some typical elements in prepared films. The changes in elemental composition can show if the reagents were deposited on the wafer surfaces. Fig. 6 depicts the XPS scan survey spectra of RTIL films with different heat treatment and some characteristic elements spectra. These spectra show the characteristic elements of IL-OH, in particular: F1s at 685.1 eV (c), N1s at 400.2 eV (d), P2p at 134.7 eV (e), were observed obviously. As shown in Fig. 6b, there are two peaks arising from C1s XPS spectrum. The first peak at 284.6 eV is assigned to the CH_2 group in IL-OH, while the second peak at 286.7 eV might originate from the C atoms bonded to the N atoms ($\text{C}^*\text{-N}$) [35]. All these indicate that

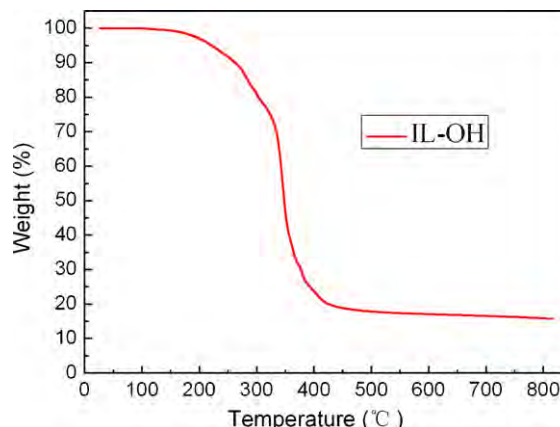


Fig. 5. TGA curve of IL-OH.

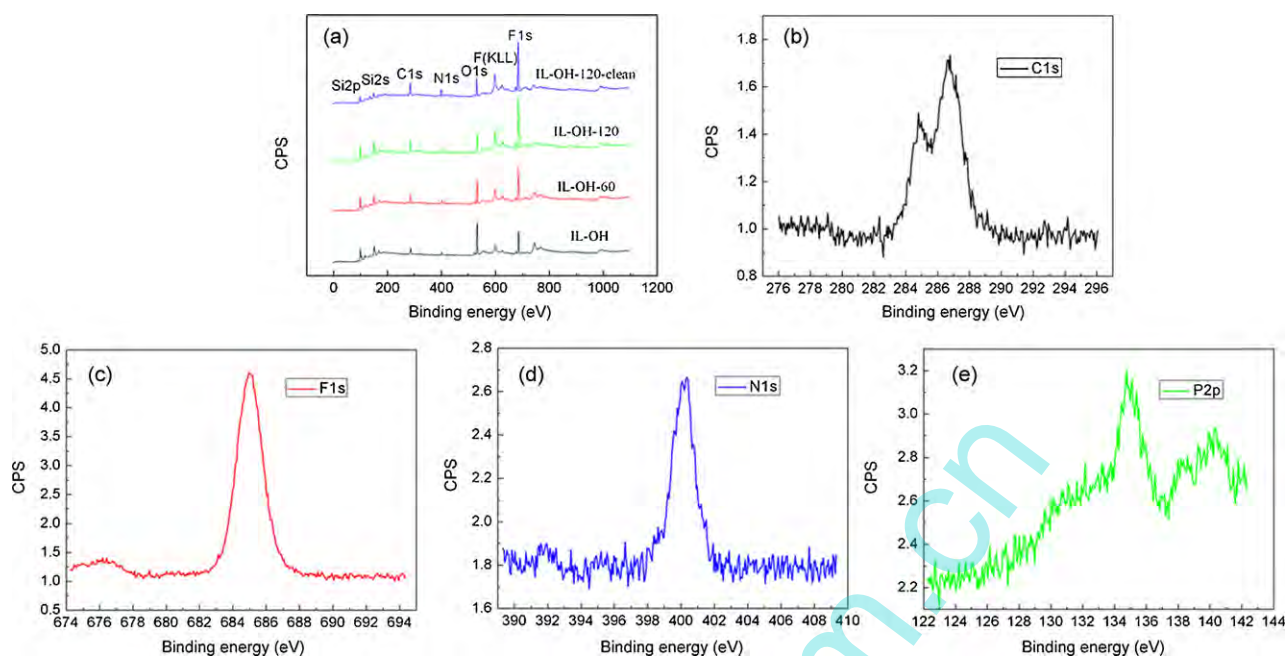


Fig. 6. XPS spectra of (a) IL-OH films with different heat treatment; (b) IL-OH-C1s; (c) IL-OH-F1s; (d) IL-OH-N1s; (e) IL-OH-P2p.

RTIL were coated successfully on the silicon surface. Meanwhile, it appears that heat treatment leads to bonding of the RTIL with Si–OH surface because some coating is left after washing with acetone [6]. This is confirmed by the spectra of IL-OH-120-clean. We can see that all the characteristic elements appear in the spectra. It is also observed that from IL-OH, IL-OH-60, IL-OH-120 to IL-OH-120-clean, the peak height of elements of F1s, N1s, and C1s increases in the sequence, but the one of Si2p, O1s decrease, the detail information was shown in Table 1. It implies that RTIL films with heat treatment become denser on the silicon surface.

AFM morphological images of IL-OH (a, b), IL-OH-60 (c, d), IL-OH-120 (e, f) and IL-OH-120-clean (g, h) films are presented in Fig. 7. As seen from Fig. 7a and b, the IL-OH film generated on the silicon surface at room temperature is not quite uniform and continuous film. There are some aggregates on the silicon surface. But after heat treatment and rinsed in acetone, IL-OH-120-clean film (Fig. 7g and h) becomes smooth on the silicon surface. IL-OH molecules distributed as small droplet in nanometer scale evenly on the silicon surface. A careful comparison of the morphologies found for RTIL films with different heat treatment suggests that the number of aggregates on the silicon surface decreased with the increase of heat temperature and after cleaning. This phenomenon seems to correspond to the amount of the mobile fraction of RTIL films where a reduction of mobile fraction can be supposed due to heat treatment and cleaning.

3.3. Adhesive force measurements under ambient conditions

Pull-off forces were measured by AFM/FFM to determine adhesive forces. Fig. 8 summarizes the adhesive forces measured on the

Table 1

The elemental composition (atom%) of RTIL films with different heat treatment.

Peak/Sample	IL-OH	IL-OH-60	IL-OH-120	IL-OH-120-clean
F1s	20.6	27.9	32.8	36.1
O1s	33.4	24.2	20.5	17.8
N1s	3.6	5.4	6.0	6.8
C1s	13.9	19.4	21.7	23.7
P2p	0.9	1.6	2.4	3.0
Si2p	27.6	21.5	16.6	12.7

RTIL films with different heat treatment, Si (100) data are provided for comparison. As shown in Fig. 8, IL-OH-120-clean showed the smallest adhesive force, whereas Si–OH exhibited the biggest adhesive force. The adhesive force decreased in the sequence of Si–OH, IL-OH, IL-OH-60, and IL-OH-120, to IL-OH-120-clean. In other words, the adhesive force has been observed to increase in the following order: fully bonded < partially bonded < untreated. Hence the adhesive force is related to the molecular packing density of the film formed on the silicon surface. In this particular case it is related to the heat treatment.

It is well known that, disordered and hydrophilic lubricant films are easily formed a meniscus by themselves or the adsorbed water molecules, resulting in higher adhesive force. In turn, hydrophobic and ordered lubricant films show low adhesion [36,37]. Another factor which affects the adhesion property is: the mobile fraction on the untreated sample IL-OH is easily forming a meniscus, which increases the tip–sample adhesion. RTIL films without being heat treated or treated at 60 °C might not form densely packed, highly uniform, and fully bonded film, water is adsorbed easily to the film surface from the environment, hence show bigger adhesive force. Conversely, the sample with no mobile lubricant fraction available (fully bonded) has the lowest adhesive force [23,24]. After heat treatment, IL-OH tends to form densely packed, more uniform, and fully bonded films, accordingly, surface with no mobile fraction IL-OH-120-clean (fully bonded) has the smallest adhesive force. In summary, according to the results reported in Section 3.4, the nano-adhesion properties of the film is closely related to the bonding fraction of the molecules on the silicon surface, which caused by the heat treatment.

3.4. Nano-tribological properties

To investigate the nano-friction properties of RTIL films with different heat treatment, the friction force versus normal load curves were measured by AFM/FFM at various normal loads and are depicted in Fig. 9. It is observed from Fig. 9 that all the films which contain IL-OH exhibit lower friction values compared to the uncoated silicon. The nano-friction force increases from IL-OH-60, IL-OH-120, IL-OH, IL-OH-120-clean, to Si–OH. IL-OH-60 has the lowest friction values and IL-OH-120-clean has the largest fric-

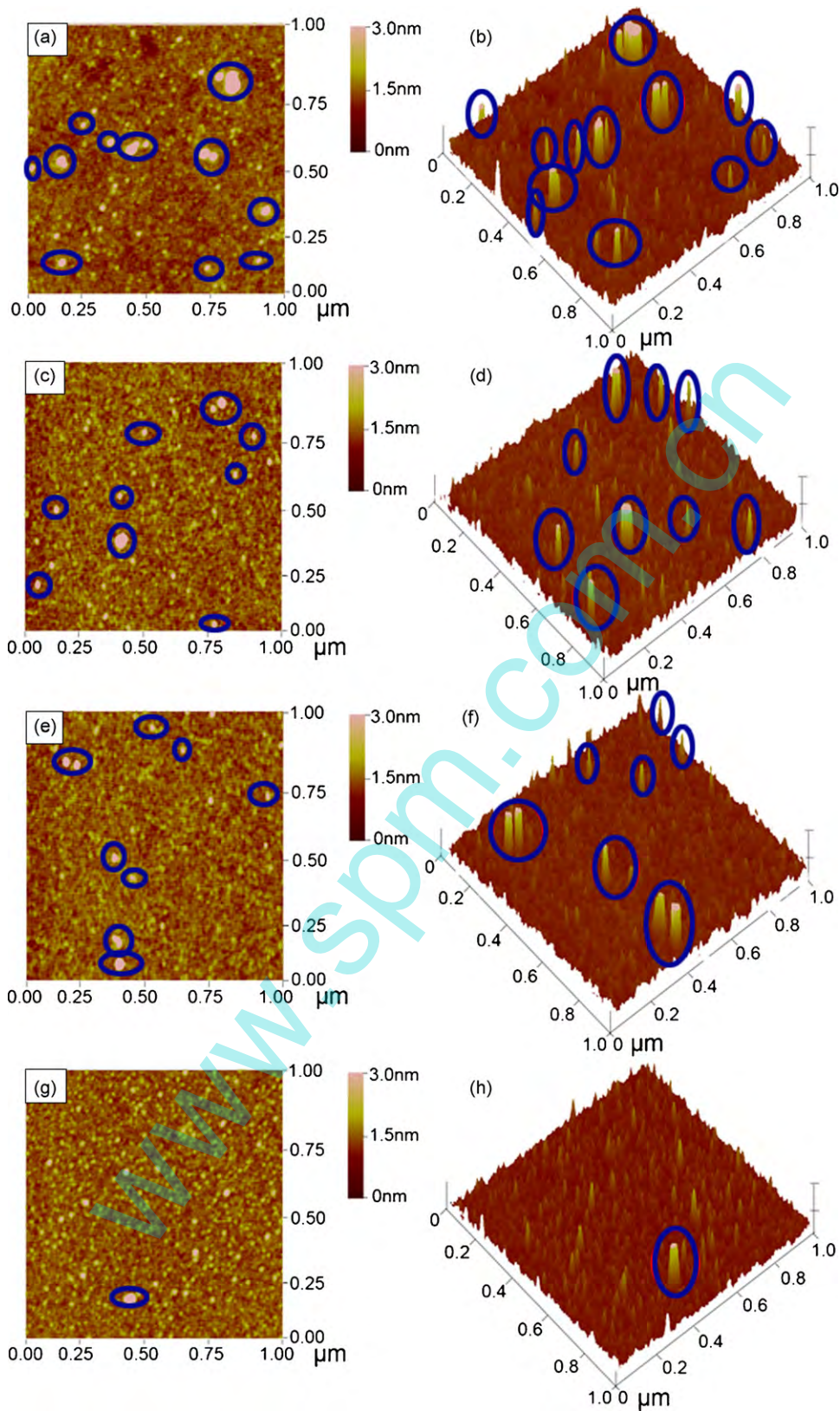


Fig. 7. 2D and 3D AFM images of (a, b) film of IL-OH; (c, d) film IL-OH-60; (e, f) film IL-OH-120; (g, h) film IL-OH-120-clean with the same Z-scale (0–3 nm).

tion values among the RTIL films but still significantly lower than Si–OH.

The difference in nano-friction can be attributed to the different bonding fraction of RTIL which caused by heat treatment. The heat treatment effect observed in the present investigation agrees

with the published literature [23]. RTIL binds to the hydroxylated silicon surface via the condensation reaction of the functional OH-groups of the RTIL-cation with hydroxylated silicon surface which is shown in Fig. 10. At room temperature, the bonding fraction between IL-OH and substrate is very little. The interaction between

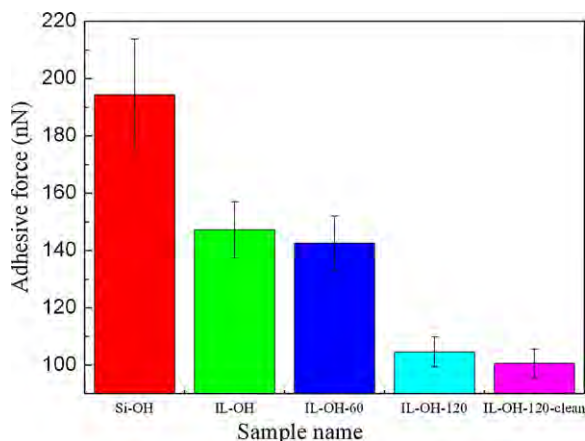


Fig. 8. Adhesion force curves of Si, IL-OH, IL-OH-60, IL-OH-120, IL-OH-120-clean films.

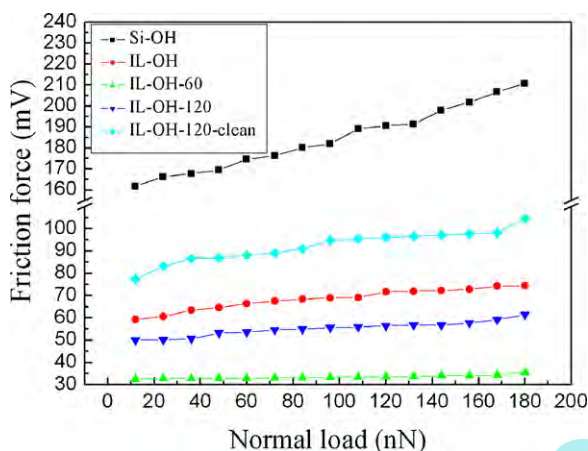


Fig. 9. Plots of nano-friction force versus applied loads for Si, IL-OH, IL-OH-60, IL-OH-120, IL-OH-120-clean films at a frequency of 1 Hz.

the lubricant and the substrate is weak, there is no (almost no) bonded RTIL causing direct contact between tip and silicon surface, leading to higher friction values. So friction values for the untreated samples (IL-OH) are larger than the data for the heat treated coat-

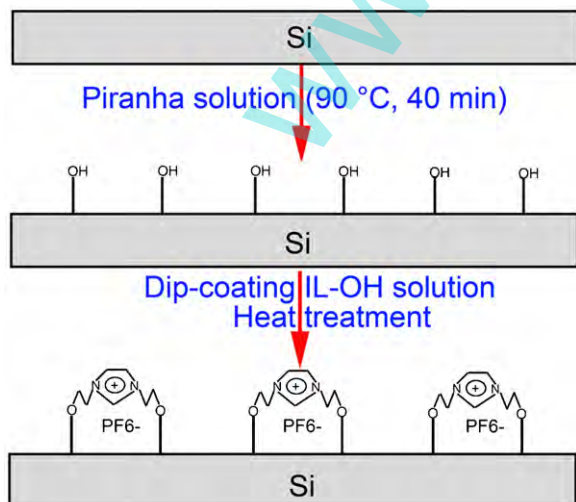


Fig. 10. Schematic diagram of IL-OH film formation.

ings. After heated at 60 °C for 1 h, IL-OH molecule binds stronger to silicon, bonding and mobile fraction reach a suitable degree. The mobile lubricant fraction present in the partially bonded samples facilitates sliding of the tip on the surface; it can rotate with the tip sliding direction easily. Accordingly, IL-OH-60 shows the lowest nano-friction force. Compared to IL-OH-60, IL-OH-120 heated at 120 °C for 1 h, bonding fraction reaches the highest point and mobile fraction reach the lowest point, hence, IL-OH-120 shows higher nano-friction. After sonicated in acetone for 20 min, IL-OH-120-clean nearly has no mobile fraction, so it shows the largest nano-friction force among the tested RTIL films. On the other hand, the film becomes more close packed with heat treatment, this can be confirmed by 2D and 3D AFM morphologies and the increasing of peak intensity (F1s, N1s and C1s) in XPS spectra. Briefly, with suitable heat treatment, bonding fraction and mobile fraction will reach an optimal proportion, leading to lower adhesion force and nano-friction force.

3.5. Micro-friction and wear properties

The wear-resistance ability of RTIL is very important for their potential use as a lubricant layer. The wear-resistance property of the films mentioned above was tested on a ball-on-plate microtribometer. Fig. 11a–d shows the plot of friction coefficients with sliding time of IL-OH RTIL films with different heat treatment.

For IL-OH film, as shown in Fig. 11a, the average friction coefficient was about 0.11 at the normal load of 60 mN. When the normal load was increased to 100 mN, the average friction coefficient decreased to about 0.1 and remained stable even after sliding for 3600 s. When the normal load was increased to 150 mN, the average friction coefficient increased sharply to 0.6 just after sliding for 110 s, which indicated that early film failure.

As depicted in Fig. 11b, the anti-wear ability of IL-OH film was enhanced greatly after being heated at 60 °C for 1 h. An average friction coefficient of 0.13 was recorded in IL-OH-60 film, and kept almost constant with increasing sliding time at a load of 60 mN. It infers that IL-OH-60 Film can remain as an effective lubricant layer for more than 3600 s at a load of 150 mN and the average friction coefficient slightly decreased to 0.09, which was still almost stable under all sliding time. However, when a load of 200 mN was applied, the film was worn out after several seconds, as witnessed by the sudden increase of the friction coefficients

Fig. 11c shows the variation of friction coefficients and durability of IL-OH-120 film on Si substrates against Si_3N_4 ball with sliding cycles respectively. It can be seen that IL-OH-120 film was recorded at an average friction coefficients about 0.2 at a load of 60 mN. With increasing normal load, durability of the RTIL films decreased dramatically, and it failed instantly at a load of 100 mN after sliding for 1960 s. Poor wear-resistance has been found for IL-OH-120-clean film. In Fig. 11d, an average friction coefficient of about 0.17 was observed in IL-OH-120-clean film at a light load of 60 mN, and the corresponding durability is only 1600 s in this case.

Bonding fraction variations induced in RTIL films by heat treatment were found to strongly influence their friction properties. From above results, it was observed that the RTIL films with appropriate bonding percentages, such as IL-OH-60 exhibited lower friction coefficient and longer durability and load-bearing capacity than higher bonding percentages (IL-OH-120 and IL-OH-120-clean) and unbonded films (IL-OH) in the test range of the load. The microtribological results nicely correspond with the findings by AFM/FFM. The enhanced friction reduction and load-carrying ability of IL-OH-60 film should rely on its intrinsic structure. The mobile uplayer and rigid underlayer of IL-OH-60 films enhanced the stability and load-bearing capacity of the entire film. Briefly,

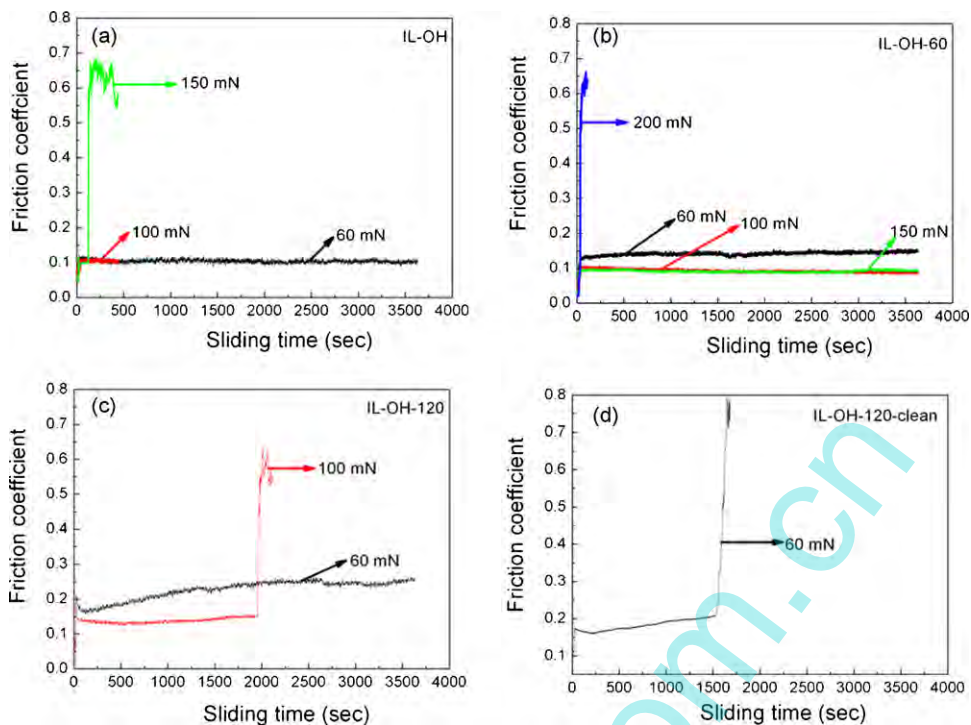


Fig. 11. Variation in friction coefficient with time for RTIL films with different heat treatment at different applied loads and a sliding frequency of 1 Hz: (a) film IL-OH; (b) film IL-OH-60; (c) film IL-OH-120; (d) film IL-OH-120-clean.

the experimental observations presented here shed light on how to design RTIL films with good frictional performances. The structure should be composed of both a rigid part to withstand load and a mobile part to reduce surface friction force.

4. Conclusions

This study compares the properties of four kinds of films based on the same RTIL, 1,3-di(2-hydroxyethyl)imidazolium hexafluorophosphate but with different heat treatment including IL-OH, IL-OH-60, IL-OH-120, and IL-OH-120-clean. Surface morphologies and XPS results indicated that different proportions of bonded and mobile RTIL films were formed due to different heat treatment condition. Adhesion and micro/nano-tribological properties of these films were investigated. IL-OH-60 films on silicon surface showed excellent friction reduction properties. Further, the mobile lubricant fraction present in the partially bonded samples facilitates sliding of the tip on the surfaces; it can rotate with the tip sliding direction easily and hence the film with higher mobile lubrication fraction exhibits the best nano-tribological performance. Heat treatment significantly changed friction and adhesion performance of the four kinds of films. Micro-friction data indicated that the dual-layer structure which contains both a rigid part to carry the applied load and a mobile part to reorganize them into original state under sliding can help to improve the film quality, reduce the friction coefficient and significantly enhance their durability and load-carrying capacity.

Acknowledgements

We are grateful to the National Natural Science Foundation of China (NSFC 50675217 & 20773148) and Innovative Group Foundation (50721062) for supporting this study.

References

- [1] H.S. Ahn, P.D. Cuong, S.K. Park, Y.W. Kim, J.C. Lim, Effect of molecular structure of self-assembled monolayers on their tribological behaviors in nano- and microscales, *Wear* 255 (2003) 819–825.
- [2] R. Maboudian, W.R. Ashurst, C. Carraro, Tribological challenges in micromechanical systems, *Tribol. Lett.* 12 (2002) 95–100.
- [3] H.S. Zhang, K. Komvopoulos, Surface modification of magnetic recording media by filtered cathodic vacuum arc, *J. Appl. Phys.* 106 (2009) 093504.
- [4] S.M. Hsu, Nano-lubrication: concept and design, *Tribol. Int.* 37 (2004) 537–545.
- [5] B. Bhushan, T. Kasai, G. Kulik, L. Barbieri, P. Hoffmann, AFM study of perfluoroalkylsilane and alkylsilane self-assembled monolayers for anti-stiction in MEMS/NEMS, *Ultramicroscopy* 105 (2005) 176–188.
- [6] M. Palacio, B. Bhushan, Ultrathin wear-resistant ionic liquid films for novel MEMS/NEMS applications, *Adv. Mater.* 20 (2008) 1194–1198.
- [7] J. Choi, H. Morishita, T. Kato, Frictional properties of bilayered mixed lubricant films on an amorphous carbon surface: effect of alkyl chain length and SAM/PPFE portion, *Appl. Surf. Sci.* 228 (2004) 191–200.
- [8] H.W. Liu, B. Bhushan, Nanotribological characterization of molecularly thick lubricant films for applications to MEMS/NEMS by AFM, *Ultramicroscopy* 97 (2003) 321–340.
- [9] S.K. Sinha, M. Kawaguchi, T. Kato, F.E. Kennedy, Wear durability studies of ultrathin perfluoropolyether lubricant on magnetic hard disks, *Tribol. Int.* 36 (2003) 217–225.
- [10] T. Kato, M. Kawaguchi, M.M. Sajjad, J. Choi, Friction and durability characteristics of ultrathin perfluoropolyether lubricant film composed of bonded and mobile molecular layers on diamond-like carbon surfaces, *Wear* 257 (2004) 909–915.
- [11] G. Caporiccio, L. Flabbi, G. Marchionniand, G.T. Viola, The properties and applications of perfluoropolyether lubricants, *J. Synth. Lubr.* 6 (1989) 133–149.
- [12] S. Mori, W. Morales, Tribological reactions of perfluoroalkyl polyether oils with stainless steel under ultrahigh vacuum conditions at room temperature, *Wear* 132 (1989) 111–121.
- [13] S. Mivake, M. Wang, S. Ninomiya, Nanotribological properties of perfluoropolyether-coated magnetic disk evaluated by vertical and lateral vibration wear tests, *Surf. Coat. Technol.* 200 (2006) 6137–6154.
- [14] C.F. Ye, W.M. Liu, Y.X. Chen, L.G. Yu, Room temperature ionic liquids: a kind of novel versatile lubricant, *Chem. Commun.* 1 (2001) 2244–2245.
- [15] X.Q. Liu, F. Zhou, Y.M. Liang, W.M. Liu, Tribological performance of phosphonium based ionic liquids for an aluminum-steel system and opinions on lubrication mechanism, *Wear* 261 (2006) 1174–1179.
- [16] H.Z. Wang, Q.M. Lu, C.F. Ye, W.M. Liu, Z.J. Cui, Friction and wear behaviors of ionic liquid of alkylimidazolium hexafluorophosphates as lubricants for steel/steel contact, *Wear* 256 (2004) 44–48.

- [17] M.H. Yao, Y.M. Liang, Y.Q. Xia, F. Zhou, X.Q. Liu, High-temperature tribological properties of 2-substituted imidazolium ionic liquids for Si₃N₄-steel contacts, *Tribol. Lett.* 32 (2008) 73–79.
- [18] I. Minami, Ionic liquids in tribology, *Molecules* 14 (2009) 2286–2305.
- [19] Z.G. Mu, F. Zhou, S.X. Zhang, Y.M. Liang, W.M. Liu, Effect of the functional groups in ionic liquid molecules on the friction and wear behavior of aluminum alloy in lubricated aluminum-on-steel contact, *Tribol. Int.* 38 (2005) 725–731.
- [20] N.S. Tambe, B. Bhushan, Scale dependence of micro/nano-friction and adhesion of MEMS/NEMS materials, coatings and lubricants, *Nanotechnology* 15 (2004) 1561–1570.
- [21] Y. Bo, F. Zhou, Z.G. Mu, Y.M. Liang, W.M. Liu, Tribological properties of ultra-thin ionic liquid films on single-crystal silicon wafers with functionalized surfaces, *Tribol. Int.* 39 (2006) 879–887.
- [22] M. Zhu, J. Yan, Y.F. Mo, M.W. Bai, Effect of the anion on the tribological properties of ionic liquid nano-films on surface-modified silicon wafers, *Tribol. Lett.* 29 (2008) 177–183.
- [23] B. Bhushan, M. Palacio, B. Kinzig, AFM-based nanotribological and electrical characterization of ultrathin wear-resistant ionic liquid films, *J. Colloid. Interface Sci.* 317 (2008) 275–287.
- [24] G.X. Xie, Q. Wang, L.N. Si, S.H. Liu, G. Li, Tribological characterization of several silicon-based materials under ionic-liquids lubrication, *Tribol. Lett.* 36 (2009) 247–257.
- [25] W.J. Zhao, M. Zhu, Y.F. Mo, M.W. Bai, Effect of anion on micro/nano-tribological properties of ultra-thin imidazolium ionic liquid films on silicon wafer, *Colloids Surf. A* 332 (2009) 78–83.
- [26] W.J. Zhao, Y.F. Mo, J.B. Pu, M.W. Bai, Effect of cation on micro/nano-tribological properties of ultra-thin ionic liquid films, *Tribol. Int.* 42 (2009) 828–835.
- [27] M. Zhu, Y.F. Mo, W.J. Zhao, M.W. Bai, Micro/macrotribological properties of several nano-scale ionic liquid films on modified silicon wafers, *Surf. Interface Anal.* 41 (2009) 205–210.
- [28] Y.F. Mo, W.J. Zhao, M. Zhu, M.W. Bai, Nano/microtribological properties of ultrathin functionalized imidazolium wear-resistant ionic liquid films on single crystal silicon, *Tribol. Lett.* 32 (2008) 143–151.
- [29] Y.F. Mo, B. Yu, W.J. Zhao, M.W. Bai, Microtribological properties of molecularly thin carboxylic acid functionalized imidazolium ionic liquid film on single-crystal silicon, *Appl. Surf. Sci.* 255 (2008) 2276–2283.
- [30] F.D. Joan, P.B. Jean, Grafted ionic liquid-phase-supported synthesis of small organic molecules, *Tetrahedron Lett.* 42 (2001) 6097–6100.
- [31] L.C. Branco, J.N. Rosa, J.J. Moura Ramos, C.A.M. Alfons, Preparation and characterization of new room temperature ionic liquids, *Chem. Eur. J.* 8 (2002) 3671–3677.
- [32] Y.S. Shon, S. Lee, RC Jr., S.S. Perry, T.R. Lee, Spiroalkanedithiol-based SAMs reveal unique insight into the wettabilities and frictional properties of organic thin films, *J. Am. Chem. Soc.* 122 (2000) 7556–7563.
- [33] S. Lee, Y.S. Shon, RC Jr., R.L. Guenard, T.R. Lee, S.S. Perry, The influence of packing densities and surface order on the frictional properties of alkanethiol self-assembled monolayers (SAMs) on gold: a comparison of sams derived from normal and spiroalkanedithiols, *Langmuir* 16 (2000) 2220–2224.
- [34] S. Yang, H. Zhang, S.M. Hsu, Correction of random surface roughness on colloidal probes in measuring adhesion, *Langmuir* 23 (2007) 1195–1202.
- [35] S.L. Ren, S.R. Yang, Y.P. Zhao, T. Yu, X.D. Xiao, Preparation and characterization of an ultrahydrophobic surface based on a stearic acid self-assembled monolayer over polyethyleneimine thin films, *Surf. Sci.* 546 (2003) 64–74.
- [36] S.H. Kim, D.B. Asay, M.T. Dugger, Nanotribology and MEMS, *Nano Today* 2 (2007) 22–29.
- [37] B. Bhushan, *Handbook of Micro/Nano Tribology*, 2nd ed., CRC Press, Boca Raton, FL, 1999.